ELSEVIER

Seminars in
ULTRASOUND
CT and MRI

Differential Diagnosis of T2 Hyperintense Brainstem Lesions: Part 1. Focal Lesions

Juan A. Guzmán-De-Villoria, MD,* Pilar Fernández-García, MD,† and Concepción Ferreiro-Argüelles, MD‡

Brainstem lesions can be classified as focal or diffuse. Magnetic resonance imaging is the most suitable imaging modality for evaluating these lesions. As a rule, focal lesions are not large and have well-defined margins. Causes include tumors, vascular malformations, demyelinating diseases, brain abscesses, hypertrophic olivary degeneration, and dilated Virchow–Robin spaces. Differential diagnoses of these numerous entities mandates a review of magnetic resonance imaging findings in conjunction with epidemiologic aspects, clinical features, and other medical test results.
Semin Ultrasound CT MRI 31:246-259

Magnetic resonance imaging (MRI) is the most sensitive and specific technique for diagnosing disorders of the posterior fossa and the brainstem (BS) in particular. Visualization of this area of the body by computed tomography (CT) is difficult because of the presence of bone-hardening artifacts.[1] Entities visible in the BS are highly diverse in their natures as well as treatment and prognosis,[1] and they can often pose a challenge for radiologists. The object of this article is to list diagnostic guidelines focusing on key imaging, epidemiologic, and clinical features as an aid to arriving at differential diagnoses of BS lesions visualized by MRI.

To this end, BS lesions have been divided into 2 main groups, focal and diffuse, with each group being considered separately in the following 2 articles. Lesion margin was the imaging criterion used for classification because focal lesions have a well-defined border. As a rule such lesions are small, affecting only a single segment of the BS. The proposed classification of BS lesions is intended to help facilitate diagnosis by using this relatively simple imaging criterion, readily discernible by radiologists but relatively nonspecific, hence as a result each group encompasses a range of different disorders.

The list of pathologic entities set forth in this and the following discussion is not intended to be exhaustive but rather to be sufficiently ample to cover most of the lesions likely to affect the BS (Table 1 and Fig. 1). Additionally, classification as a focal or diffuse lesion is determined on the basis of MRI findings, and hence one and the same disorder, such as gliomas, can fall within both of these proposed groupings.

Focal BS Tumors

This group includes tumors having well-defined margins affecting at least one half of the BS segment in which they are located, although they may extend longitudinally into a single adjacent segment provided that the margins remain well defined and that the tumor compresses and displaces, rather than infiltrates, the adjacent cerebral parenchyma.[2]

Patient age is the first factor to be considered when diagnosing a focal BS tumor. Gliomas are the most common neoplasm in children, comprising nearly 90% of tumors of the BS during childhood.[3] These tumors may be located in any part of the BS but are most commonly found in the midbrain and the medulla.[3] Where the midbrain is affected, involvement of the ventral portion, ie, the cerebral peduncle, is rare.[4,5] Certain locations are highly characteristic, for example, tectal gliomas (Fig. 2A) and gliomas of the cervicomedullary junction with posterior exophytic expansion into the fourth ventricle or below the cerebellum.[3,6]

Clinical findings for patients vary with tumor location. Accordingly, focal midbrain gliomas located in the tectum will give

*Department of Radiology/Neuroradiology, Hospital General Universitario "Gregorio Marañón," Madrid, Spain.
†Department of Radiology/Neuroradiology, Hospital General Universitario "Gregorio Marañón," Madrid, Spain.
‡Department of Radiology, Hospital "Severo Ochoa," Leganés, Madrid, Spain.
Address reprint requests to: Juan A. Guzmán-De-Villoria, Department of Radiology/Neuroradiology, Hospital General Universitario "Gregorio Marañón," Madrid, Spain, c/o Dr. Esquedo 46, 28007 Madrid, Spain. E-mail: jguzman.hgugm@salud.madrid.org

 0887-2171/10/$-see front matter
doi:10.1053/j.sult.2010.03.001

Table 1 Conclusions of Focal BS Lesions That Are Hyperintense on T2-Weighted Imaging

Entity	Epidemiology	Clinical Symptoms	Location	Key MRI Findings	Other Particulars
Focal glioma	Children: 5-10 years old 90% BS tumors are gliomas Adults: 40-60 years old <2% of all gliomas	Indefinite depending on location	Children: midbrain and medulla. Cervicomedullary junction (exophytic). Tectal plate Adults: pons. Tectal plate	Nonenhancing in children Enhancement and necrosis in adults	Tectal tumors benign in appearance and course in children and young adults
PNET	<3 years old	Indefinite depending on location	Pons	Nonenhancing	Dissemination via CSF
Dermoid/epidermoid tumors	All ages, very rare	Indefinite, variable Aseptic meningitis	Prepontine cistern invading the pons	Signal similar to CSF on T1 and T2 Hyperintense on FLAIR ↓ ADC Nonenhancing	
Metastasis	>45 years old 3%-5% of all brain metastases	Indefinite depending on location	Nonspecific	Multiple, necrosis, enhancement, bleeding, edema	
Arterial infarctions	>45 years old plus cardiovascular risk factors, heart disease, vascular dissection, or dolichoectasia	Indefinite depending on location	Anteromedial, anterolateral, lateral, posterior vascular territories Deep lesion where affected vessel is small	Morphology depending on vascular territory ↓ ADC 0-14 d	High proportion of false negatives on DWI in first 24 h
DVA	20-50 years old 50%-60% of all vascular malformations (2%-3% in BS)	Mostly asymptomatic	Adjacent to fourth ventricle, brachium pontis or dentate nucleus	Dilated medullary veins (caput medusae) converging on a single drainage vein	Associated with CM (more frequently) or capillary telangiectasia
CM	30 years old 5%-10% of all vascular malformations (18%-35% in BS)	Recurring-remitting clinical symptoms	Pons > midbrain > medulla	"Popcorn-like" structure Hyperintense center on T1 and T2 (methemoglobin) Hypointense margins on T2 (hemosiderin)	Multiple CMs in sporadic and familial forms
Capillary telangiectasia	In adults	Mostly asymptomatic	Pons	<2 cm. Single. Slightly hyperintense on T2 Moderate, stippled enhancement Hypointense on T2*GE	Magnetic susceptibility caused by deoxyHb in ectasic vessels
AVM	20-30 years old 2%-6% of all intracranial AVMs	Acute clinical situation due to bleeding	Midbrain > pons > medulla	Abnormal vessels exhibit signal void or hyperintense on T1 and/or T2 where there is turbulent flow or thrombosis	Hemorrhagic signs where bleeding occurs
MS	15-45 years old	Recurring-remitting clinical symptoms	Floor of fourth ventricle or surface of pons	Small lesions Active lesions are enhancing	Lesser tendency to form "black holes" on T1 Less hyperintense on T2, less well defined than supratentorial lesions
ADEM	Children and young adults Infection or vaccination 1-3 wks earlier	Preceded by pseudoinfluenza symptoms Recurring clinical symptoms Monophasic (+ Fr.) or multiphasic (MDEM)	Nonspecific	Single or multiple lesions variable in size May be enhancing ↓ ADC for acute lesions	Concomitant involvement of cerebellum, basal ganglia or thalamus Periventricular cerebral white matter spared (≠ MS)
Abscesses	All ages	Indefinite depending on location cranial nerve pair VI and VII involvement	Pons	Ring-shaped uptake vasogenic edema ↓ ADC except tuberculosis MRS: lactate, succinate, amino acids	Rule out primary focus of infection in paranasal, sinuses, middle ear, or teeth
HOD	All ages	Palatal tremor Nystagmus Hypermetropic or torsional saccades	ION: -ipsilateral (CTT lesion) -contralateral (DN or SCP lesion) -bilateral (SCP and CTT lesion)	ION hyperintense on T2 > 3-4 weeks-indefinitely Hypertrophy ION 6 mo to 3/4 years Nonenhancing	Triggering lesions Atrophy of cerebellar cortex and contralateral DN

Table 1 Continued

Entity	Epidemiology	Clinical Symptoms	Location	Key MRI Findings	Other Particulars
Dilated VR Spaces	Advanced age	Asymptomatic Sometimes hydrocephalus	Region: • pontomesencephalic • midbrain-diencephalic • midbrain-thalamus	Signal similar to CSF on all sequences	May be multiseptate Gliosis sometimes produces peripheral hyperintense on T2

ADC, apparent diffusion coefficient; ADEM, acute disseminated encephalomyelitis; AVM, arteriovenous malformation; BS, brainstem; CM, cavernous malformation; CSF, cerebrospinal fluid; CTT, central tegmental tract; DeoxyHb, deoxyhemoglobin; DN, dentate nucleus; DVA, developmental venous anomaly; DWI, diffusion-weighted Imaging; GE, gradient echo; HOD, hypertrophic olivary degeneration; ION, inferior olivary nucleus; MDEM, acute multiphasic encephalomyelitis; MRS, MR spectroscopy; MS, multiple sclerosis; PNET, primitive neuroectodermal tumor; SCP, superior cerebellar peduncle; VHL, von Hippel–Lindau; VR, Virchow–Robin.

rise to signs of hydrocephalus, namely, headache, vomiting, and papilledema. Gliomas located in the tegmentum will cause dysfunction of the oculomotor nuclei and their connecting fibers. Signs of ataxia will be present in the case of extension towards the superior cerebellar peduncle.[4,5] Gliomas located in the cervicomedullary junction will exhibit signs of lower cranial nerve and pyramidal tract involvement.[5]

Nonenhancement is an imaging finding that is very useful in differentiating this type of lesion from other forms of neoplasm or even from pseudotumors.[4,6] However, although an absence of enhancement is the norm, there are exceptions.[5] Enhancement in these cases may be ringlike or spotty, a finding that has been associated with aggressive tumors.[3] Exophytic cervicomedullary gliomas are a special case in which, characteristically, peripheral enhancement is seen with enhancement of the solid parts of the tumor even though they are low-grade astrocytomas.[6]

Primitive neuroectodermal tumors (PNETs) are another type of neoplasm that can be found in children. This tumor diagnosis should be considered in children younger than 3 years,[7] whereas tumors in children who are a little older, between 5 and 10 years of age, tend to be gliomas.[6] PNETs are most commonly located in the pons, where, unlike PNETs located elsewhere, these lesions are not usually enhancing.[7] This diagnosis must be considered when leptomeningeal dissemination through the CSF is detected.[7]

Epidermoid/dermoid tumors of the BS are rare; only 12 cases described in the literature have been located in the BS,[8] with one half of these cases presenting in children. The clinical findings that have been described are nonspecific, and patients may be asymptomatic or, conversely, may exhibit prominent deficits and/or recurrent meningitis.[8] Location in the pontine cistern with intraaxial invasion of the adjacent portion of the pons is a radiological feature that is rather suggestive of this type of lesion.[8] This behavior is thought to be related to the nature of these lesions, which, as remnants of embryonic ectodermal tissue, are considered to spread intraaxially along Virchow–Robin spaces. Their imaging features are similar to those of the other epidermoid cysts of the

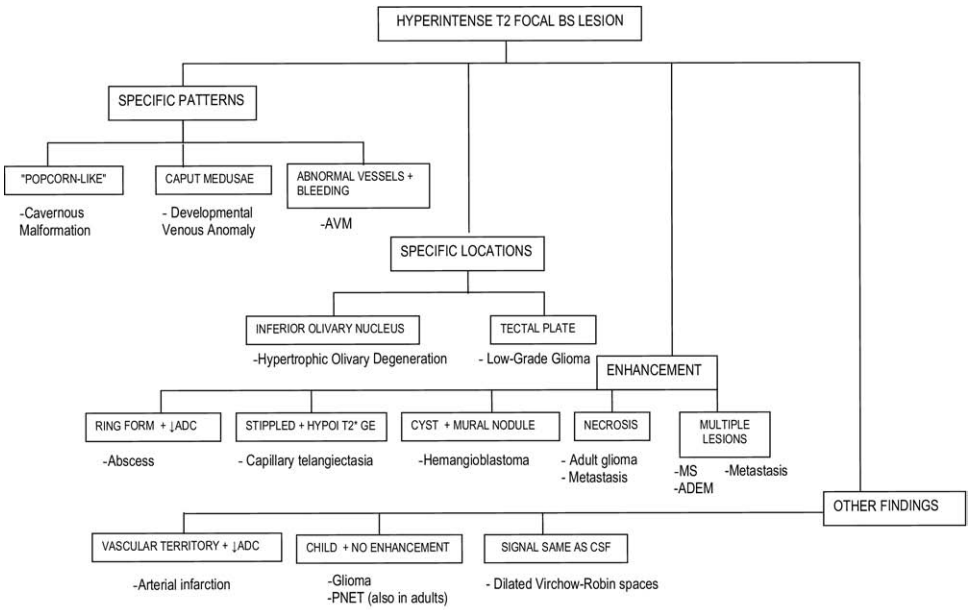

Figure 1 Differential diagnostic algorithm for focal BS lesions that are hyperintense on T2-weighted imaging. ADC, apparent diffusion coefficient; ADEM, acute disseminated encephalomyelitis; AVM, arteriovenous malformation; BS, brainstem; CSF, cerebrospinal fluid; GE, gradient echo; Hypoi, hypointensity; MS, multiple sclerosis; PNET, primitive neuroectodermal tumor.

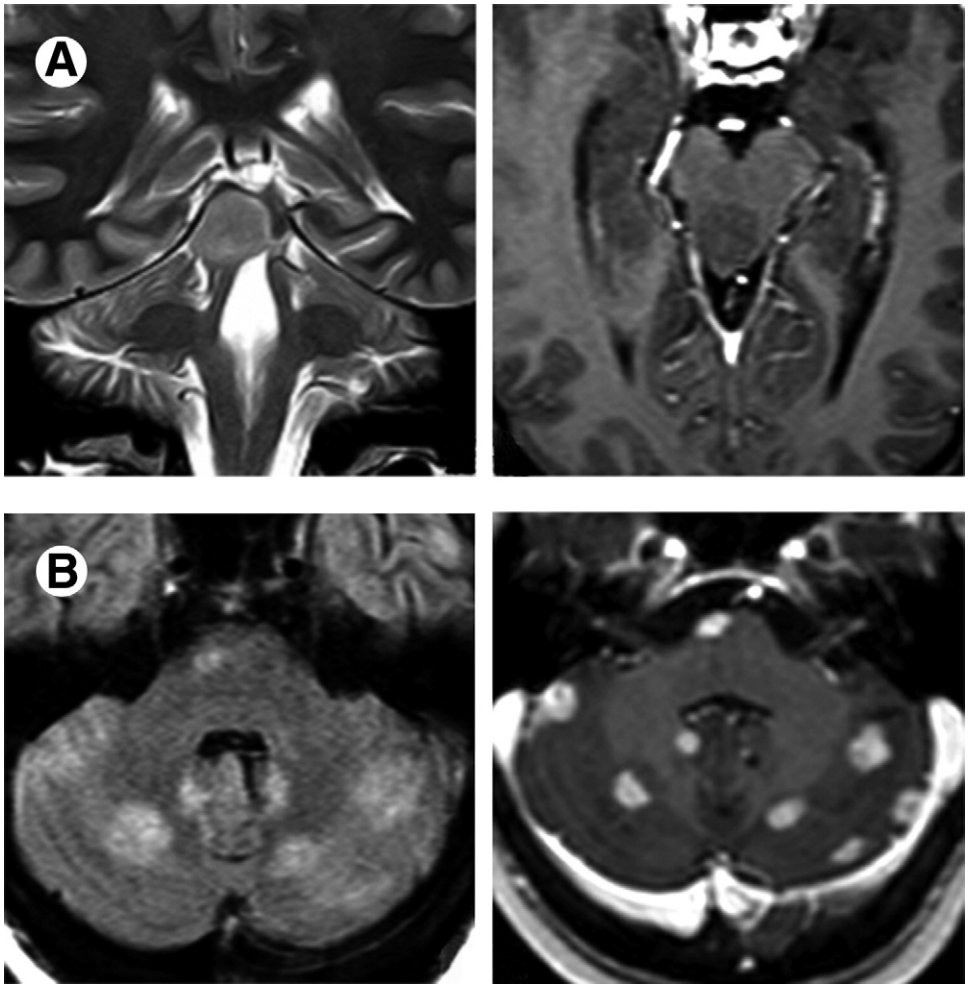

Figure 2 (A) Tectal glioma. Coronal T2-weighted image (left) shows a well-circumscribed, slightly hyperintense mesencephalic tectal and tegmental mass. Axial gadolinium T1-weighted image (right) demonstrates expansion into the mesencephalic tegmentum on the right side by a sharply delineated hypointense mass. No enhancement is present. (B) Multiple metastases (breast adenocarcinoma). Axial FLAIR (left) shows pontine hyperintense round focal lesion without edema. Multiple similar lesions can be seen at gray-white matter junction in both cerebellar hemispheres. Axial gadolinium T1-weighted image (right) shows ring-enhancing lesions.

posterior fossa: they have multilobulated borders and a signal like that of cerebrospinal fluid (CSF) on T1- and T2-weighted sequences and signal hyperintensity on fluid attenuation inversion recovery (FLAIR) sequences.[9] They are nonenhancing after administration of gadolinium chelating agents and display restricted diffusion.[10]

Unlike the situation in children, the vast majority of tumor lesions that will be identified in the BS in adults will display enhancement. Metastasis is one of the initial diagnoses to be considered because of relative frequency. The actual incidence of brain metastases is not accurately known, although postmortem examinations have shown metastasis to be present in 24% of cancer deaths.[11] Incidence increases with age, chiefly after age 45.[12] Metastases in the BS account for approximately 3% to 5% of all brain metastases.[13] Imaging findings in the BS are similar to those in other locations. The presence of multiple lesions and imaging signs of aggressiveness (necrosis, enhancement, bleeding, and edema) and a medical history of a known primary tumor can help guide a diagnosis (Fig. 2B).

Hemangioblastoma must be considered when evaluating young adult/middle-aged patients. On average, the age at diagnosis of this type of neoplasm ranges between 40 and 55 years of age.[14] This benign tumor accounts for 1.1% to 2.4% of all tumors of the nervous system and 7.3% of all tumors of the posterior fossa in adults.[15] There are several key features that are helpful in diagnosis. Lesions often have epicenter at the area postrema of the medulla oblongata,[15,16] that is, near the floor of the fourth ventricle. There is a pathognomonic radiological finding: identification of a cystic lesion with a mural nodule fed by enlarged blood vessels.[15] Instead of a cyst, there may be a cavity (syringobulbia),[15] similar to the large syringomyelic cavities that may be found in spinal hemangioblastomas.[17] Variations on these imaging findings may also arise. For instance, the macroscopic blood vessels seen in magnetic

resonance (MR) may not be visualized in tumors smaller than 10 to 15 mm.[15,17] Initially, this type of tumor begins as a solid growth with strong enhancement followed by the appearance of an internal enlarging cyst that increases in size until a nodule can be seen around the peripheral portion of the predominant cyst.[18]

It should be noted that between 5% and 30% of hemangioblastomas are associated with von Hippel–Lindau disease (VHL).[16] This autosomal-dominant genetic disorder may be suspected on the basis of family history or radiological findings. The presence of multiple hemangioblastomas in the posterior fossa or medulla is more common in these patients, and other cranial or extracranial pathologies may also be present (retinal hemangioblastomas, renal cysts or carcinomas, pancreatic cysts, or papillary cystoadenoma of the epididymis).[16] Endolymphatic sac tumors are also quite characteristic. Hemangioblastoma onset occurs some 10 to 15 years earlier in VHL patients than in patients with sporadic hemangioblastomas.[14]

Contrary to the situation in children, BS gliomas are uncommon in adults. They comprise fewer than 2% of all gliomas,[19] and of these, approximately 40% can be considered focal.[20] Generally speaking, the pons is the most common location.[20] This type of tumor comprises 2 groups. Group 1 is composed of malignant adult gliomas of the BS. This type of tumor appears as a mass with generally peripheral enhancement and necrosis. Histologically, they are anaplastic astrocytomas or oligodendrocytomas with a poor prognosis. They ordinarily present in patients older than 40 years of age, primarily in patients in their 60s.[20] Group 2 are focal tectal gliomas. They are identical in appearance to their counterparts in children. Identification of these tumors is based on their location, in these lesions are clearly confined within the tectal plate, sometimes evincing posterior exophytic growth;[6] their benign appearance (no necrosis, hemorrhage, or enhancement); and their indolent course.[20] Clinical symptoms feature hydrocephalus.[6]

Arterial Infarction

BS infarction accounts for approximately 10%[21,22] of brain infarcts. Accordingly, in view of the high incidence and prevalence of ischemic brain lesions in the general population, infarcts will be one of the most frequent entities encountered in the BS. Patients presenting with this type of disorder are generally older than 45 years of age[23,24] with cardiovascular risk factors (arterial hypertension, diabetes mellitus, a smoking habit, hyperlipidemia), heart disease requiring anticoagulant therapy (atrial fibrillation, patent foramen ovale, etc.), or a vascular pathology of the vertebrobasilar system, such as vertebral/basilar artery dissections or dolichoectasias.[24,25] Arterial hypertension is the vascular risk factor most commonly associated with BS infarction[22] and is present in up to 68% to 73% of cases.[21,24,25]

Arterial infarcts may appear in any BS segment, with the pons being most frequently involved, followed by the medulla and then the midbrain.[21,22] As a rule these patients present with clinical features consistent with acute neurological deficit depending on lesion topography, and hence features are highly variable.[24-26] From an imaging standpoint, it is important to assess lesion morphology and location, with the distribution of lesions being associated with the different vascular territories, which can be grouped into 4 regions[27]: anteromedial, anterolateral, lateral, and posterior. The surface and morphology of each of these areas varies according to the level that is examined. Generally speaking, these territories have well-defined borders on either side on the basis of imaginary lines drawn from the anterior surface to the posterior surface of the BS. Anteromedial lesions do not extend past the midline, although it should be borne in mind that bilateral infarction is not uncommon in this territory.[25] It also needs to be considered that in most cases infarcts will affect several territories[24,25,28] and will extend cranially or caudally into other BS segments or even into other tributary structures of the posterior circulation, such as the cerebellum, thalamus, or occipital lobes.[25]

However, the lesions produced by the occlusion of very small perforating vessels are very small (<15 mm) deep lacunar infarcts[24,25] with highly nonspecific MR findings. These lacunar infarcts account for most ischemic lesions of the BS.[21,24,25]

In all cases where ischemic brain infarction is suspected, it is essential to perform diffusion-weighted imaging (DWI) sequences. The findings will depend on the time elapsed from the onset of clinical symptoms (Fig. 3A and B). A reduction in apparent diffusion coefficient (ADC) values can be seen in as little as 3 hours after onset,[21] a finding that is highly specific for acute infarction. However, greater proportions of false-negative results have been recorded for diffusion studies in the first 24 hours in cases of acute infarction of the posterior circulation, and particularly of the BS.[29] Therefore, FLAIR sequences may visualize lesions but not demonstrate restriction of diffusion soon after clinical onset.[29] In cases like this, it is advisable to repeat the MR scan 24 hours after the acute event to increase the sensitivity of the diffusion sequences.[29]

The high percentage of false-negative results in the BS obtained by the use of DWI is thought to be attributable to low spatial resolution for detecting small lacunar infarcts and magnetic susceptibility artifacts present in the posterior fossa on the echo-planar sequences commonly used in diffusion studies.[29,30] This behavior is also thought to be ascribable firstly to the fact that BS neurons are more ischemia resistant and secondly to the existence of a well-developed network of collateral perforating vessels in this region.[21]

When MR is not performed until more than 14 days after the acute event, ADC values may be similar to those for healthy tissue,[31] a phenomenon known as “pseudonormalization” produced by concomitant vasogenic and cytotoxic edema. In such cases it should be noted that the infarct identified on the T2-weighted or FLAIR sequences exhibits increased signal intensity on DWI,[31] even though ADC maps are not revealing.

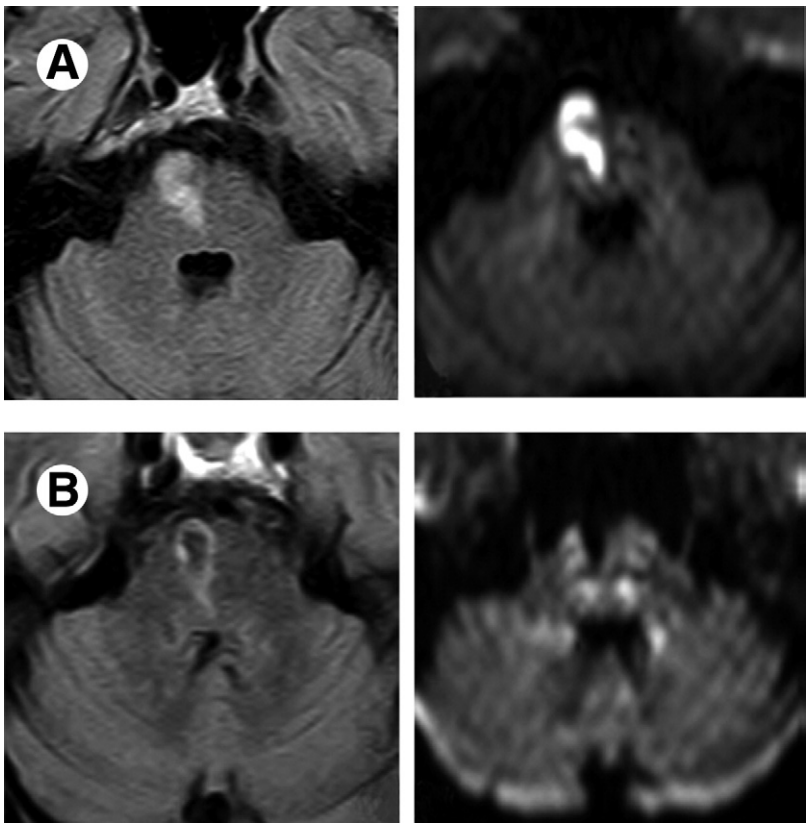

Figure 3 (A) Acute infarct. Axial FLAIR (left) shows a hyperintense wedge-shaped right anteromedial pontine lesion. Axial DWI (right) reveals hyperintense restricted diffusion (cytotoxic edema). (B) Chronic infarct. Axial FLAIR (left) shows a low signal in the malacic area with a hyperintense gliotic area at the margins. DWI (right) reveals no evidence of restricted diffusion.

Vascular Malformations

Four types of vascular malformations in the central nervous system are commonly described: venous angioma or developmental venous anomaly (DVA), cavernoma or cavernous malformation (CM), capillary telangiectasia, and arteriovenous malformation (AVM).[32,33] All occur in the BS, but fortunately diagnosis on the basis of MRI findings is usually possible.

DVA is the most frequent vascular malformation, accounting for 50% to 63% of all vascular malformations and reported to be present in 2.5% of postmortem examinations.[34] Approximately 2% to 3% of cases are found in the BS.[34] This entity usually appears in patients between the ages of 20 and 50.[34] In most cases, DVAs are asymptomatic, although associations with neurological clinical symptoms, such as seizures, headache, and neurological deficits, or abnormalities caused by the mass effect, for instance, hydrocephalus caused by obstruction of the aqueduct of sylvius, have also been described.[34-36] By contrast, DVAs do not exhibit signs of complications like rupture or hemorrhage.[36]

On MRI, DVAs exhibit a characteristic appearance. They consist of a network of dilated medullary veins, conventionally known as caput medusae because of the resemblance in their appearance, converging on a single, or sometimes multiple, enlarged drainage vein.[34] This abnormality generally exhibits low signal intensity on T1-weighted images, and the drainage vein may display signal hyper or hypointensity on T2-weighted sequences depending on the flow rate, orientation, or pulse sequence used.[35] DVA is clearly identified on sequences with obtained with intravenous contrast, which reveal enhancement by the abnormal venous structures.[34,35]

In some cases, and particularly on T2-weighted images, the dilated drainage vein may stand out more than the small vascular structures comprising the caput medusae (Fig. 4A).[34] In these cases it may be helpful to review the location and direction of the drainage veins, which will ordinarily be the veins one would expect on the basis of normal venous anatomy. Therefore, because DVAs in the BS are usually located adjacent to the fourth ventricle, in the brachium pontis (or middle cerebellar peduncle) or the dentate nucleus,[34] the drainage veins are as follows: (1) anterior transpontine vein, which crosses the pons along the midline from the subependymal region of the fourth ventricle; (2) lateral transpontine vein, which follows a path similar to that of the preceding vein but is in a more lateral position; (3) vein of the lateral recess of the fourth ventricle, running towards the

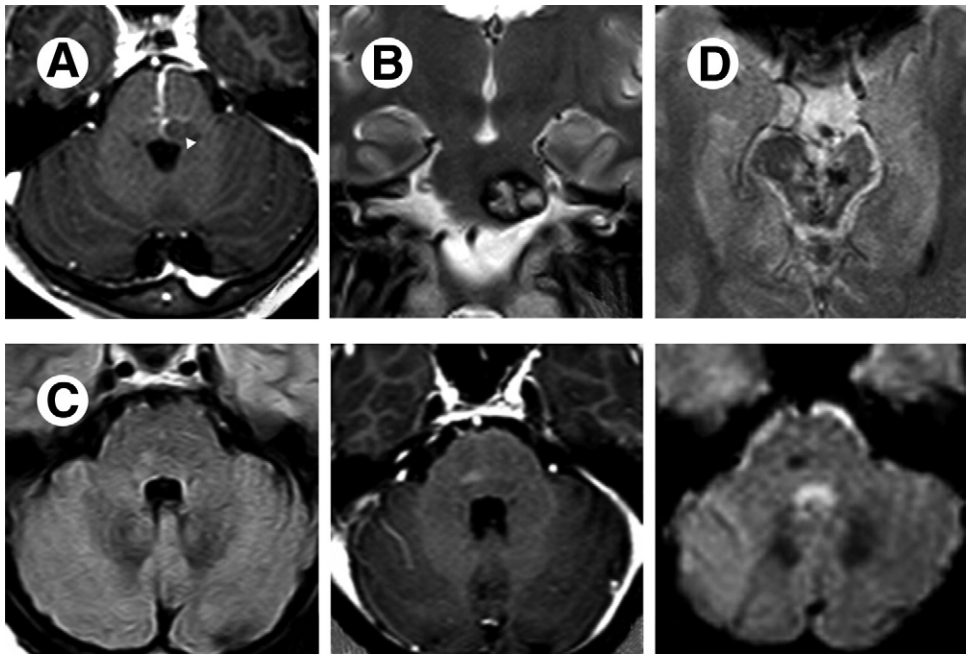

Figure 4 (A) Venous angioma and cavernous malformation. Axial gadolinium-enhanced 3D FFE-T1 shows stellate, tubular vessels (caput medusae/"Medusa's head") from the fourth ventricle floor converging on a dilated left pontine collector vein draining into the dural sinus. Coexisting cavernous malformation is frequent as shown (arrowhead). (B) Cavernous malformation. Coronal turbo spin echo (TSE) T2 shows a reticulated "popcorn-like" lesion in the left hemipons with a mixed signal core and hypointense hemosiderin rim. (C) Capillary telangiectasia. Axial FLAIR (left) shows stippled foci of hyperintensity in the right pons. Axial gadolinium T1-weighted image (middle) demonstrates faint stippled enhancement of the lesion. Axial DWI (FFE-EPI T2*) (right) reveals a poorly defined hypointense lesion. (D) Arteriovenous malformation. Axial FFE-T2 shows a "honeycomb" of multiple flow voids in the mesencephalic region typical of arteriovenous malformation and a surrounding high signal due to gliosis. Note marked midbrain atrophy.

anterior pial surface of the pons-brachium pontis from the lateral recess of the fourth ventricle; (4) longitudinal intra tegmental vein running longitudinally in the tegmentum of the pons and the midbrain parallel to the aqueduct; and (5) deep medullary veins running to the lateral recesses of the fourth ventricle from the brachium pontis or dentate nucleus.[34]

The prevalence of cavernous malformation in the general population is 0.4% to 0.9%,[37] approximately 18% to 35% located in the BS.[38] CM accounts for 5% to 10% of all malformations of the central nervous system.[39] Unlike other vascular malformations, such as DVA and capillary telangiectasias, there is a clear association between this vascular malformation and the presence of neurological deficits resulting from the affected BS nuclei and pathways.[38-41] This is because over its natural course, CM has a tendency to bleed, estimated at 2.4% to 6% patient/year,[38,40,41] a risk that increases to 21% to 60% in cases of rebleeding.[39-41] Because of this behavior clinical, onset tends to be acute, after which there is ordinarily a period of recovery or possibly a succession of episodes of relapse or new symptoms caused by rebleeding, simulating clinical episodes of recurrence and remission like those commonly identified in multiple sclerosis (MS).[41] This type of malformation usually first manifests itself clinically at around 30 years of age.[38,40,41]

The typical cavernoma has what has been described as a "popcorn-like" or "mulberry-like" appearance on MR thanks to the existence of multiple hemorrhages in differing stages (Fig. 4B). It thus takes the form of a nodular lesion with areas of heterogeneous high-signal lesions on T1- and T2-weighted sequences, surrounded by a circular or irregularly shaped region of low signal intensity on T2-weighted images caused by hemosiderin deposited around the bright methemoglobin signal.[41] Edema is only present in the event of acute hemorrhage and subsides after a few days.[41] These general findings may vary depending on the type of bleeding. Accordingly, Zabramski et al[42] described 4 types of CM. Type I lesions have a hyperintense core on T1 spin echo (SE) sequences and a hyper or hypointense core on T2 SE. These cavernomas exhibit signs of subacute bleeding. The signal for type II lesions indicates a reticulated mixed core on T1 SE sequences, whereas T2 SE images reveal the same reticulated mixed core appearance together with a hypointense ring. These lesions have areas of bleeding and thrombosis of several years duration. Type III lesions are iso- or hypointense on T1 SE sequences and hypointense on T2 SE images, but they have a markedly hypointense ring that magnifies the lesion. In these cases there are signs of chronic bleeding with hemosiderin within and surrounding the lesion. Type IV lesions are small CMs visible only on T2*gradient echo (GE)

sequences. CMs are located most frequently in the pons (57%), followed by the midbrain (25%) and the medulla (18%).[40] Multiple CMs are detected in 24% to 33% of sporadic forms and in 75% of familial forms.[41,43]

On the basis of postmortem studies, the prevalence of capillary telangiectasias is 0.4%,[44] and they comprise 16% to 20% of all vascular malformations.[45] They appear more frequently in adults, which suggests an acquired origin.[32,46] In most cases, lesions are asymptomatic, and it is not yet clear whether there are any relevant associated clinical findings.[45,47,48]

These lesions are most frequently located in the pons.[32,44,47] They tend to be single lesions,[32,44] small in size, generally smaller than 2 cm.[44] In most cases, they cannot be detected on T1-weighted sequences and may be iso- or mildly hyperintense on T2-weighted images and DP.[44] Administration of contrast medium yields a uniform or "stippled" appearance.[32,44] The margins of the enhancement zone are irregular, imparting what has been termed a "brush-like" appearance.[32] The findings are thus nonspecific and similar to those for such diverse entities as MS, infarcts, CPM, and neoplasms.[32,48] However, the characteristic finding for capillary telangiectasias is loss of signal intensity on T2*GE images (Fig. 4C).[32,44] Magnetic susceptibility of deoxyhemoglobin in the ectasic vessels of this malformation has been postulated as the cause, because anatomopathological studies have revealed neither blood residues nor calcium.[32,44] However, T2*GE scans are not sufficiently sensitive to demonstrate loss of signal intensity for some, mainly small, capillary telangiectasias. In these cases DWI has been shown to afford greater detection sensitivity.[47]

Other useful findings include the absence of mass effect and stability of lesions on follow-up imaging.[32,44] This type of vascular malformation has recently been reported to exhibit signal hypointensity on susceptibility-weighted imaging.[49]

Mixed vascular malformations are frequently observed. The concurrence of cavernomas and DVAs is especially common.[50] Associations between capillary telangiectasias and DVAs or CMs have also been described, and indeed an association among CM, DVA, and capillary telangiectasia has even been reported.[50,51] The findings in these cases are a combination of the findings described for each of the associated vascular malformations. They may be situated some distance apart or very close together.

AVMs in the BS comprise 2% to 6% of all intracranial AVMs.[52] They mostly tend to be symptomatic because of the high likelihood of hemorrhage, approximately of 70% to 90% overall and 15.1% annually.[52] Indeed, 80% to 90% of these AVMs present with intracranial hemorrhage.[53] Although this entity may appear at any age, mean age at presentation is approximately 20 to 30 years of age, and AVMs are most frequently located in the midbrain, followed by the pons and the medulla.[52,53]

The appearance of AVMs in the BS in MR scans is similar to the appearance in the rest of the central nervous system and in most cases is readily recognizable. Imaging reveals abnormally dilated, overdeveloped vascular structures with "flow void" phenomena caused by signal loss produced by high flow rates. An increased signal can also be obtained because of turbulent flow in the vessels or vessel thrombosis. Signs of bleeding will be seen in the case of ruptured AVMs (Fig. 4D).

Multiple Sclerosis

The BS is frequently involved at the time of clinically isolated syndrome on presentation of MS,[54] and it has been estimated that 35% of patients presenting with clinically isolated syndrome with BS involvement will develop clinically definite MS.[55] Furthermore, lesions are commonly found in the BS in patients who have already received a diagnosis of MS. For instance, in a series of 114 cases published by Ormerod et al,[56] 68% of patients with clinically definite MS had lesions in the BS.

Sequence selection is important in this context. For instance, conventional SE and fast spin echo T2-weighted image acquisition has been shown to be more sensitive than fast-FLAIR imaging for detecting posterior fossa lesions.[57,58] Some authors have ascribed this behavior to lower T2 signal values for posterior fossa lesions compared with white matter lesions. These differences in the T2 signal values have been attributed to the structure of the closely packed fibers of the BS.[54]

MS lesions in the BS tend to be located primarily on the floor of the fourth ventricle and on the surface of the pons.[54] Similar to lesions within the supratentorial compartment, they may exhibit gadolinium enhancement. These lesions are typically more diffuse and less hyperintense than their supratentorial counterparts.[54] Furthermore, they are less likely to form "black holes" of pronounced signal hypointensity on T1-weighted sequences.[59]

As a rule, areas of demyelination in the BS tend to be small,[59] but large abnormalities do occur that may be confused with tumors, chiefly gliomas.[60,61] However, acute lesions of the BS do not usually develop cysts or an exophytic component.[60]

Demonstrating typical supratentorial MS lesions, specifically in the periventricular white matter and the callosal-septal sulcus (Fig. 5), are other findings that may be helpful in reaching a diagnosis. Also, the reader should be aware of another demyelinating disease, neuromyelitis optica (also known as Devic's disease) that selectively affects the optic nerve and spinal cord while sparing the brain.[62] In this case there may be BS involvement without supratentorial lesions.

Additionally, it may also be helpful to consider lesion development because the lesions may increase in size or conversely shrink until they virtually disappear. Disease stage and progression would then be indicated by the appearance of new lesions.

Age at onset of MS is an epidemiological factor to consider. MS is ordinarily diagnosed at ages of between 15 and 45 years,[63] and hence a diagnosis of MS is not to be expected in children, who comprise fewer than 3% of cases.[60] Oligoclonal bands in the CSF are more commonly seen in cases of MS with lesions in the BS.[54] In the case of neuromyelitis

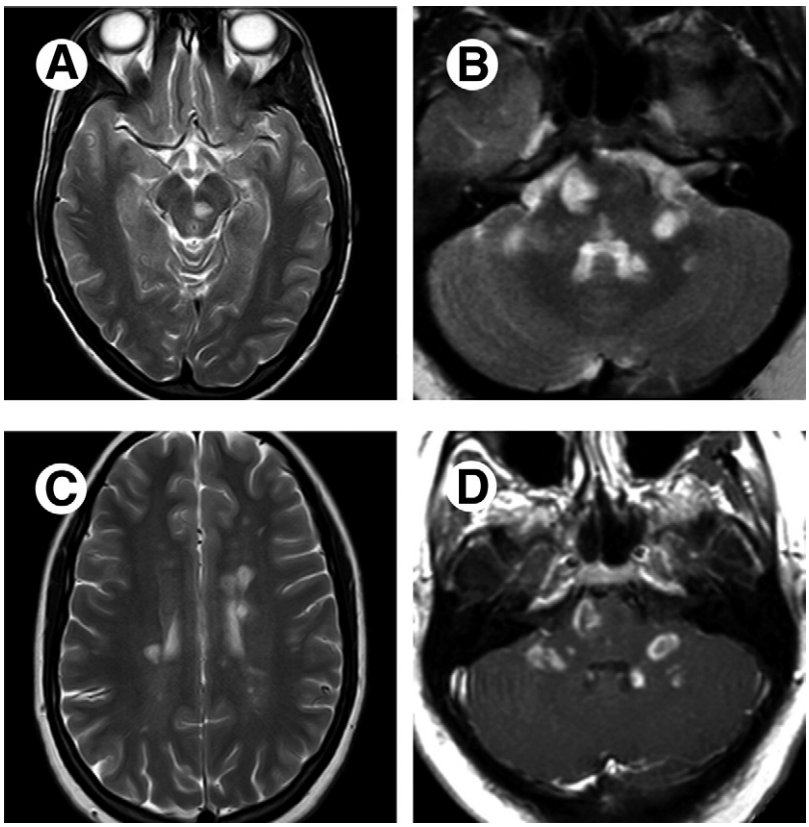

Figure 5 MS. Axial TSE T2-weighted image (A) shows increased focal signal in the left mesencephalic red nucleus. Axial TSE-T2 (B) shows multiple hyperintense periventricular focal lesions on the anterior surface of the pons and in both middle cerebellar peduncles. Axial TSE T2-weighted image (C) reveals multiple hyperintense focal lesions perpendicular to the long axis of the lateral ventricles. Axial gadolinium-enhanced 3D FFE-T1-weighted image (D) shows nodular, complete and incomplete ringlike enhancement patterns.

optica, the blood antibody NMO-IgG has a 90% specificity rate.[62]

Acute Disseminating Encephalomyelitis

Acute disseminating encephalomyelitis (ADEM) is a generally monophasic multifocal inflammatory disease of the central nervous system, in most cases preceded by infection or vaccination 1 to 3 weeks before clinical onset.[64] BS involvement is characterized by single or multiple lesions variable in size which may enhance with intravenous contrast.[65] The MRI abnormalities of ADEM are quite similar to those produced by MS, and these 2 diseases can be indistinguishable.[66,67] Differential diagnosis between these 2 entities is determined on the basis of clinical, MR, and laboratory test results. From an epidemiologic standpoint, ADEM is usually diagnosed in children and young adults,[66] whereas MS occurs in childhood only infrequently.[68] Most cases present a systemic clinical picture of pseudoinfluenza starting 4 to 21 days after the triggering event which precedes the neurological symptoms.[67] Unlike MS, classically ADEM is a monophasic disease, but even so remitting-recurring cases have been reported, and in such cases it is termed multiphasic disseminated encephalomyelitis.[68] Clinical neurological features may be the same as for MS, although with certain particularities: clinical features similar to encephalopathy are more frequent in ADEM, affecting the level of consciousness and giving rise to epileptic seizures or meningismus.[68] The presence of bilateral optic neuritis and complete transverse myelitis has also been described in children,[67] which may differentiate this entity from encephalitis.[69]

In MR scans, involvement of the BS together with the cerebellum, basal ganglia, and thalamus is more frequent in ADEM than in MS.[67,68] Although the abnormalities caused by ADEM have sometimes been described as being confined to the BS, more commonly there is concomitant involvement of other areas.[65] Lesions ordinarily affect brain structures bilaterally but asymmetrically and are variable in size,[68] with a tendency for lesions to be large and irregular in shape.[70] Furthermore, in contrast to MS, demyelination zones ordinarily spare the corpus callosum and the periventricular white matter.[67,68] Hemorrhage within the lesions is infrequent but, where it occurs, may suggest a diagnosis of ADEM.[70,71]

In the series reported by Atzori et al,[68] with a mean follow-up of 6.8 years, more than 50% of the lesions remitted fully in children with ADEM, whereas in the rest the lesions underwent a pronounced reduction. By con-

trast, in patients with MS, new lesions accrue in 80% of cases.

Acute ADEM lesions may give rise to restriction on DWI, enabling the lesions to be differentiated from chronic lesions.[72] A decrease in ADC values has also been related to a poor prognosis for patients with lesions in the BS.[73] The pathophysiology underlying this behavior on diffusion-weighted sequences is unknown, but the cause has been postulated to be swelling of damaged oligodendrocytes or increased cellularity ensuing from inflammatory infiltrates, or it may even be a subtype of vasculitic disorder.[72,73] By contrast, ADEM lesions are unlikely to be confused with acute ischemic lesions, which also exhibit restricted diffusion, in view of the differing clinical presentations and imaging findings.

CSF analysis may help differentiate ADEM from MS. Accordingly, whereas the detection of oligoclonal immunoglobulin G bands is nearly exclusively associated with MS, a lymphocyte level greater than 30 per μL is a finding that is closely associated with ADEM.[68]

Abscess

Abscess of the BS is rare, comprising fewer than 4% of abscesses of the posterior fossa and fewer than 1% of all brain abscesses.[74,75] In contrast to conventional wisdom, clinical findings are usually not suggestive of infection, ie, in most cases there is no fever, signs of meningismus, or leukocytosis.[74-77] Consequently, patient symptoms generally result from affected BS nuclei and/or tracts. Because abscesses in the BS are most frequently located in the pons, cranial nerves VI and VII are most frequently involved.[74]

The characteristic imaging finding is the presence of a lesion displaying contrast uptake in the form of a ring with surrounding vasogenic edema.[74] On T2-weighted sequences the capsule is hypo- or isointense[74,78] with a markedly hyperintense central portion,[74] typically showing restricted diffusion.[74] This diffusion behavior is probably the result of the high viscosity of coagulative necrosis, the hypercellularity of the pus, and the binding of water molecules on the surfaces of the bacterial walls.[74,76] Low ADC values are far more typical of bacterial abscesses than those caused by tuberculosis, toxoplasmosis, or fungi.[74,76,77]

For tuberculomas, visualization of a peripheral enhancing mass with a hyposignal on T1 and T2-weighted images of the outer ring and hypointense content on T2-weighted images has been reported as characteristic.[77] Spectroscopy can be helpful in diagnosing brain abscesses. This technique can be used to identify peaks of such abnormal metabolites as lactate, acetate, succinate, and various amino acids, for example, valine and leucine, which are not present in other focal lesions, for instance, tumors.[74] Finally, identifying a primary focus of infection as the origin of a brain abscess can also be helpful, and the abscess will, by extension, be primary or metastatic.[75] The main foci are the paranasal sinuses, middle ear, and teeth.[74]

Hypertrophic Olivary Degeneration

Hypertrophic olivary degeneration (HOD) has been regarded as one form of transsynaptic degeneration in that it is associated with hypertrophy rather than atrophy of the inferior olivary nucleus (ION). The key diagnostic feature is the presence of a lesion at a distance from the ION, giving rise to a lesion in the dento-rubro-olivary pathway[79] making up the anatomical triangle of Guillain and Mollaret.[80] The red nucleus synapses with the ION via the central tegmental tract. The ION, in turn, is connected to the contralateral dentate nucleus and then to the contralateral red nucleus through the superior cerebellar peduncle.[81] Hypertensive hemorrhage is most frequently responsible for HOD,[81,82] but there is a long list of triggering factors, including tumors, demyelinating lesions, inflammation, cavernomas, and infarction.[79,81-83]

Therefore, the site of the triggering lesion in the BS determines the ION that will undergo hypertrophic degeneration. Accordingly, if the primary lesion is restricted to the central tegmental tract, HOD will be ipsilateral, whereas if there is dentate nucleus or superior cerebellar peduncle involvement, HOD will be contralateral (Fig. 6A).[81] Bilateral involvement is possible where the lesion affects both the superior cerebellar peduncle and the central tegmental tract (Fig. 6B).[79]

MR examination allows the visualization of hypertrophy and manifested high signal in the ION on T2-weighted images, but the timeline for the appearance of these 2 findings is not the same. The increase in signal intensity on T2-weighted sequences begins 3 to 4 weeks after onset of the triggering lesion and subsists indefinitely thereafter.[84,85] Olivary hypertrophy appears initially 6 months after the acute event and remits after 3 to 4 years.[84] The absence of gadolinium enhancement may also aid in differential diagnosis.[85]

Another imaging finding, but one that is less consistently present, is atrophy of the cerebellar cortex and dentate nucleus contralateral to the olive with HOD after degeneration ensuing from disruption of the olivodentate fibers.[84,85] A hyposignal on T2-weighted sequences of the contralateral dentate nucleus has also been described.[85]

Symptomatic palatal tremor, consisting of myoclonus of the levator veli palatini muscle contralateral to the hypertrophic olive is a classic clinical finding in patients with HOD. Patients may also complain of a clicking sound in the ear.[86] There may also be nystagmus or hypermetropic or torsional saccades (oculo palatal myoclonus).[86] Synchronic contractions of the cervical muscles, diaphragm, tongue and limbs have also been reported.[79,86]

Dilated Virchow–Robin Spaces

Virchow–Robin (VR) spaces surround the walls of the blood vessels entering the cerebral parenchyma from the subarach-

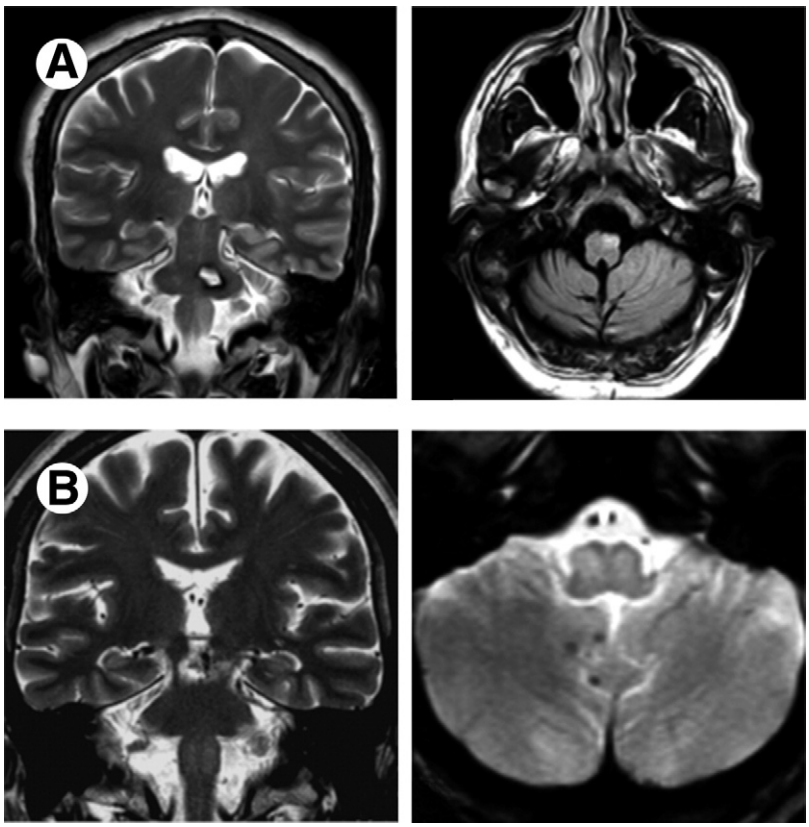

Figure 6 (A) Unilateral HOD. Coronal TSE-T2 (left) shows hyperintense focal lesion in the left ION. Note left pontine cavernoma, the primary midbrain lesion that led to ipsilateral HOD. Axial FLAIR (right) shows increased signal in left anterior medulla corresponding to the region of the ION. (B) Bilateral HOD. Coronal TSE T2-weighted image (left) shows bilateral hyperintensity confined to both IONs. Note mesencephalic AVM as primary midbrain lesion that led to bilateral HOD. Axial FFE-T2*-weigthed image (right) shows a symmetric high signal bilaterally and enlargement of the IONs secondary to midbrain hemorrhage (not shown). Note 3 hypointense punctate foci in the right cerebellar hemisphere (multiple cavernomatosis).

noid space. They can be seen in all age groups, although their frequency and size increase with advancing age.[87] These lesions are generally asymptomatic, but because of their mass effect, on occasion they do give rise to clinical symptoms like Parkinsonism or motor weakness, although hydrocephalus is the most frequent clinical syndrome because of stenosis of the aqueduct of sylvius.[88] MRI findings are characterized by a signal similar to CSF on all sequences, no gadolinium enhancement, and no restriction on diffusion imaging.[89] The location of the dilated VR spaces is of great importance in making a differential diagnosis. There are 3 types on the basis of location. Type I VR spaces follow the lenticulostriate arteries entering the basal ganglia through the anterior perforated substance. Type II VR spaces occur along the paths of the perforating medullary arteries as they extend into the gray matter and the white matter in the convexity. Type III VR spaces are located in the BS and are the type of interest to us here.[89] The most frequent location in the BS is the pontomesencephalic region, where VR spaces tend to be situated between the cerebral peduncle and the substantia nigra along the collicular artery and accessory collicular artery. In the upper BS (mesencephalo-diencephalic junction) they are located along the penetrating arteries behind the cerebral peduncle (posterior thalamoperforating or interpeduncular artery).[88] VR spaces in the midbrain-thalamus may sometimes be greatly enlarged, taking on a complex, multicystic appearance that can be associated with a mass effect and alteration of the signal from the adjacent hyperintense parenchyma on T2-weighted imaging and FLAIR sequences by reactive gliosis (Fig. 7). Because of direct compression of the third ventricle or the aqueduct of Sylvius, these lesions cause hydrocephalus.[88,90]

Conclusions

MRI is the modality most commonly used to evaluate focal lesions of the BS. Focal BS lesions are the result of a large variety of pathologic processes, including tumors, ischemia, infection, demyelinating diseases, degenerative disorders, and vascular malformations. In some cases a diagnosis may be reached solely on the basis of MRI findings for the BS lesion, but in many other cases the findings are nonspecific. In such cases other, associated abnormalities in brain structures other than the BS should be taken into account. Considering changes in the imaging findings over time or in response to a given treatment can be helpful. It is also essen-

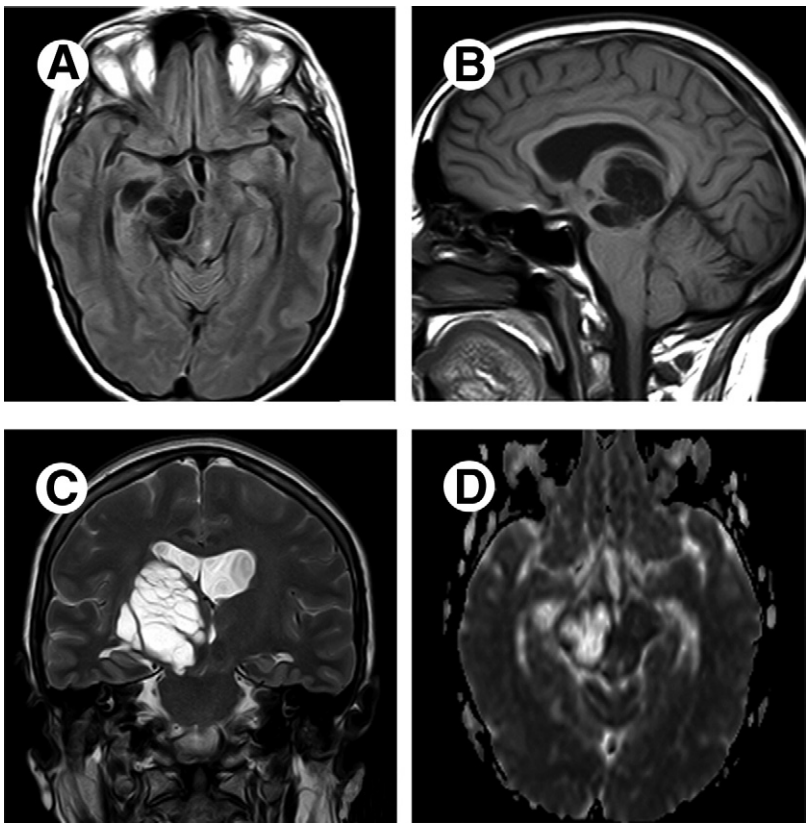

Figure 7 Enlarged VR spaces. Sagittal T1-weighted image (A) shows clusters of isointense variable-sized cysts with CSF in the midbrain. Axial FLAIR (B) shows a CSF-suppressed signal within the cysts. Coronal TSE T2-weighted imaged (C) demonstrates expansion and mass effect laterally in the third ventricle. ADC map (D) reveals increased water diffusion of the lesions.

tial to take account nonradiological aspects, such as patient age, disease incidence, clinical findings, and other test results, for instance, CSF analysis. As a consequence, in view of the differing prognoses and treatments for each of these different types of focal lesions affecting the BS, assessing MRI findings in the clinical and epidemiologic context of the patient is critical.

References

1. Gass A, Filippi M, Grossman RI: The contribution of MRI in the differential diagnosis of posterior fossa damage. J Neurol Sci 172:S43-S49, 2000 (suppl 1)
2. Barkovich AJ, Krischer J, Kun LE, et al: Brain stem gliomas: A classification system based on magnetic resonance imaging. Pediatr Neurosurg 16:73-83, 1990
3. Kwon JW, Kim IO, Cheon JE, et al: Paediatric brain-stem gliomas: MRI, FDG-PET and histological grading correlation. Pediatr Radiol 36:959-964, 2006
4. Sun B, Wang CC, Wang J: MRI characteristics of midbrain tumours. Neuroradiology 41:158-162, 1999
5. Vandertop WP, Hoffman HJ, Drake JM, et al: Focal midbrain tumors in children. Neurosurgery 31:186-194, 1992
6. Guillamo JS, Doz F, Delattre JY: Brain stem gliomas. Curr Opin Neurol 14:711-715, 2001
7. Zagzag D, Miller DC, Knopp E, et al: Primitive neuroectodermal tumors of the brainstem: Investigation of seven cases. Pediatrics 106: 1045-1053, 2000
8. Caldarelli M, Colosimo C, Di Rocco C: Intra-axial dermoid/epidermoid tumors of the brainstem in children. Surg Neurol 56:97-105, 2001
9. Obana WG, Wilson CB: Epidermoid cysts of the brain stem. Report of three cases. J Neurosurg 74:123-128, 1991
10. Tsuruda JS, Chew WM, Moseley ME, et al: Diffusion-weighted MR imaging of the brain: Value of differentiating between extraaxial cysts and epidermoid tumors. AJNR Am J Neuroradiol 11:925-931; discussion:932-924, 1990
11. Johnson JD, Young B: Demographics of brain metastasis. Neurosurg Clin North Am 7:337-344, 1996
12. Nelson JS, von Deimling A, Perersen I, et al: in Kleihues P and Cavenee WK (eds): World Health Organization Classification of Tumours: Pathology and Genetics of Tumours of the Nervous System. Lyon, IARC Publishing, 2000, p 250
13. Fuentes S, Delsanti C, Metellus P, et al: Brainstem metastases: Management using gamma knife radiosurgery. Neurosurgery 58:37-42; discussion:37-42, 2006
14. Weil RJ, Lonser RR, DeVroom HL, et al: Surgical management of brainstem hemangioblastomas in patients with von Hippel–Lindau disease. J Neurosurg 98:95-105, 2003
15. Lee SR, Sanches J, Mark AS, et al: Posterior fossa hemangioblastomas: MR imaging. Radiology 171:463-468, 1989
16. Choyke PL, Glenn GM, Walther MM, et al: Von Hippel–Lindau disease: Genetic, clinical, and imaging features. Radiology 194:629-642, 1995
17. Chu BC, Terae S, Hida K, et al: MR findings in spinal hemangioblastoma: Correlation with symptoms and with angiographic and surgical findings. AJNR Am J Neuroradiol 22:206-217, 2001
18. Slater A, Moore NR, Huson SM: The natural history of cerebellar hemangioblastomas in von Hippel–Lindau disease. AJNR Am J Neuroradiol 24:1570-1574, 2003
19. White HH: Brain stem tumors occurring in adults. Neurology 13:292-300, 1963

20. Guillamo JS, Monjour A, Taillandier L, et al: Brainstem gliomas in adults: Prognostic factors and classification. Brain 124:2528-2539, 2001
21. Toi H, Uno M, Harada M, et al: Diagnosis of acute brain-stem infarcts using diffusion-weighed MRI. Neuroradiology 45:352-356, 2003
22. Bogousslavsky J, Van Melle G, Regli F the Lausanne Stroke Registry: Analysis of 1,000 consecutive patients with first stroke. Stroke 19: 1083-1092, 1988
23. Roh JK, Kim KK, Han MH, et al: Magnetic resonance imaging in brainstem ischemic stroke. J Korean Med Sci 6:355-361, 1991
24. Kim JS, Kim J: Pure midbrain infarction: Clinical, radiologic, and pathophysiologic findings. Neurology 64:1227-1232, 2005
25. Kumral E, Bayulkem G, Akyol A, et al: Mesencephalic and associated posterior circulation infarcts. Stroke 33:2224-2231, 2002
26. Schmahmann JD, Ko R, MacMore J: The human basis pontis: Motor syndromes and topographic organization. Brain 127:1269-1291, 2004
27. Tatu L, Moulin T, Bogousslavsky J, et al: Arterial territories of human brain: Brainstem and cerebellum. Neurology 47:1125-1135, 1996
28. Cho TH, Nighoghossian N, Tahon F, et al: Brain stem diffusion-weighted imaging lesion score: A potential marker of outcome in acute basilar artery occlusion. AJNR Am J Neuroradiol 30:194-198, 2009
29. Oppenheim C, Stanescu R, Dormont D, et al: False-negative diffusion-weighted MR findings in acute ischemic stroke. AJNR Am J Neuroradiol 21:1434-1440, 2000
30. Frey LC, Sung GY, Tanabe J: Early false-negative diffusion-weighted imaging in brainstem infarction. J Stroke Cerebrovasc Dis 11:51-53, 2002
31. Axer H, Grassel D, Bramer D, et al: Time course of diffusion imaging in acute brainstem infarcts. J Magn Reson Imaging 26:905-912, 2007
32. Barr RM, Dillon WP, Wilson CB: Slow-flow vascular malformations of the pons: Capillary telangiectasias? AJNR Am J Neuroradiol 17:71-78, 1996
33. Campeau NG, De Lane JI: Novo development of a lesion with the appearance of a cavernous malformation adjacent to an existing developmental venous anomaly. AJNR Am J Neuroradiol 26:156-159, 2005
34. Lee C, Pennington MA, Kenney CM, 3rd: MR evaluation of developmental venous anomalies: Medullary venous anatomy of venous angiomas. AJNR Am J Neuroradiol 17:61-70, 1996
35. Blackmore CC, Mamourian AC: Aqueduct compression from venous angioma: MR findings. AJNR Am J Neuroradiol 17:458-460, 1996
36. Giannetti AV, Rodrigues RB, Trivelato FP: Venous lesions as a cause of sylvian aqueductal obstruction: Case report. Neurosurgery 62:E1167-E1168; discussion: E1168, 2008
37. Labauge P, Brunereau L, Laberge S, et al: Prospective follow-up of 33 asymptomatic patients with familial cerebral cavernous malformations. Neurology 57:1825-1828, 2001
38. Kupersmith MJ, Kalish H, Epstein F, et al: Natural history of brainstem cavernous malformations. Neurosurgery 48:47-53; discussion:53-44, 2001
39. Ferroli P, Sinisi M, Franzini A, et al: Brainstem cavernomas: Long-term results of microsurgical resection in 52 patients. Neurosurgery 56: 1203-1212; discussion:1212-1204, 2005
40. Hauck EF, Barnett SL, White JA, et al: Symptomatic brainstem cavernomas. Neurosurgery 64:61-70; discussion:70-61, 2009
41. Wang CC, Liu A, Zhang JT, et al: Surgical management of brain-stem cavernous malformations: Report of 137 cases. Surg Neurol 59:444-454; discussion:454, 2003
42. Zabramski JM, Wascher TM, Spetzler RF, et al: The natural history of familial cavernous malformations: Results of an ongoing study. J Neurosurg 80:422-432, 1994
43. Lehnhardt FG, von Smekal U, Ruckriem B, et al: Value of gradient-echo magnetic resonance imaging in the diagnosis of familial cerebral cavernous malformation. Arch Neurol 62:653-658, 2005
44. Lee RR, Becher MW, Benson ML, et al: Brain capillary telangiectasia: MR imaging appearance and clinicohistopathologic findings. Radiology 205:797-805, 1997
45. Huddle DC, Chaloupka JC, Sehgal V: Clinically aggressive diffuse capillary telangiectasia of the brain stem: A clinical radiologic-pathologic case study. AJNR Am J Neuroradiol 20:1674-1677, 1999
46. Guibaud L, Pelizzari M, Guibal AL, et al: Slow-flow vascular malformation of the pons: Congenital or acquired capillary telangiectasia. AJNR Am J Neuroradiol 17:1798-1799; author reply:1799-1800, 1996
47. Finkenzeller T, Fellner FA, Trenkler J, et al: Capillary telangiectasias of the pons. Does diffusion-weighted MR increase diagnostic accuracy? Eur J Radiol, in press
48. Scaglione C, Salvi F, Riguzzi P, et al: Symptomatic unruptured capillary telangiectasia of the brain stem: Report of three cases and review of the literature. J Neurol Neurosurg Psychiatry 71:390-393, 2001
49. Yoshida Y, Terae S, Kudo K, et al: Capillary telangiectasia of the brain stem diagnosed by susceptibility-weighted imaging. J Comput Assist Tomogr 30:980-982, 2006
50. Pozzati E, Marliani AF, Zucchelli M, et al: The neurovascular triad: Mixed cavernous, capillary, and venous malformations of the brainstem. J Neurosurg 107:1113-1119, 2007
51. Clatterbuck RE, Elmaci I, Rigamonti D: The juxtaposition of a capillary telangiectasia, cavernous malformation, and developmental venous anomaly in the brainstem of a single patient: Case report. Neurosurgery 49:1246-1250, 2001
52. Nozaki K, Hashimoto N, Kikuta K, et al: Surgical applications to arteriovenous malformations involving the brainstem. Neurosurgery 58: ONS-270-ONS-278; discussion:ONS-278-ONS-279, 2006
53. Kurita H, Kawamoto S, Sasaki T, et al: Results of radiosurgery for brain stem arteriovenous malformations. J Neurol Neurosurg Psychiatry 68: 563-570, 2000
54. Yousry TA, Grossman RI, Filippi M: Assessment of posterior fossa damage in MS using MRI. J Neurol Sci 172:S50-S53, 2000 (suppl 1)
55. Sastre-Garriga J, Tintore M, Rovira A, et al: Conversion to multiple sclerosis after a clinically isolated syndrome of the brainstem: Cranial magnetic resonance imaging, cerebrospinal fluid and neurophysiological findings. Mult Scler 9:39-43, 2003
56. Ormerod IE, Miller DH, McDonald WI, et al: The role of NMR imaging in the assessment of multiple sclerosis and isolated neurological lesions. A quantitative study. Brain 110:1579-1616, 1987
57. Yousry TA, Filippi M, Becker C, et al: Comparison of MR pulse sequences in the detection of multiple sclerosis lesions. AJNR Am J Neuroradiol 18:959-963, 1997
58. Bastianello S, Bozzao A, Paolillo A, et al: Fast spin-echo and fast fluid-attenuated inversion-recovery versus conventional spin-echo sequences for MR quantification of multiple sclerosis lesions. AJNR Am J Neuroradiol 18:699-704, 1997
59. Gass A, Filippi M, Rodegher ME, et al: Characteristics of chronic MS lesions in the cerebrum, brainstem, spinal cord, and optic nerve on T1-weighted MRI. Neurology 50:548-550, 1998
60. Glasier CM, Robbins MB, Davis PC, et al: Clinical, neurodiagnostic, and MR findings in children with spinal and brain stem multiple sclerosis. AJNR Am J Neuroradiol 16:87-95, 1995
61. Kishimoto R, Yabe I, Niino M, et al: Balo's concentric sclerosislike lesion in the brainstem of a multiple sclerosis patient. J Neurol 255: 760-761, 2008
62. Park KY, Ahn JY, Cho JH, et al: Neuromyelitis optica with brainstem lesion mistaken for brainstem glioma. Case report. J Neurosurg 107: 251-254, 2007
63. Fadil H, Kelley RE, Gonzalez-Toledo E: Differential diagnosis of multiple sclerosis. Int Rev Neurobiol 79:393-422, 2007
64. Caldemeyer KS, Smith RR, Harris TM, et al: MRI in acute disseminated encephalomyelitis. Neuroradiology 36:216-220, 1994
65. Firat AK, Karakas HM, Yakinci C, et al: An unusual case of acute disseminated encephalomyelitis confined to brainstem. Magn Reson Imaging 22:1329-1332, 2004
66. Hartung HP, Grossman RI, ADEM: Distinct disease or part of the MS spectrum? Neurology 56:1257-1260, 2001
67. Garg RK: Acute disseminated encephalomyelitis. Postgrad Med J 79: 11-17, 2003
68. Atzori M, Battistella PA, Perini P, et al: Clinical and diagnostic aspects of multiple sclerosis and acute monophasic encephalomyelitis in pediatric patients: A single centre prospective study. Mult Scler 15:363-370, 2009
69. Harris C, Lee K: Acute disseminated encephalomyelitis. J Neurosci Nurs 39:208-212, 2007

70. Singh S, Alexander M, Korah IP: Acute disseminated encephalomyelitis: MR imaging features. AJR Am J Roentgenol 173:1101-1107, 1999
71. Tenembaum S, Chamoles N, Fejerman N: Acute disseminated encephalomyelitis: A long-term follow-up study of 84 pediatric patients. Neurology 59:1224-1231, 2002
72. Kuker W, Ruff J, Gaertner S, et al: Modern MRI tools for the characterization of acute demyelinating lesions: Value of chemical shift and diffusion-weighted imaging. Neuroradiology 46:421-426, 2004
73. Axer H, Ragoschke-Schumm A, Bottcher J, et al: Initial DWI and ADC imaging may predict outcome in acute disseminated encephalomyelitis: Report of two cases of brain stem encephalitis. J Neurol Neurosurg Psychiatry 76:996-998, 2005
74. Ramalho J, Castillo M: Case of the season: Brainstem abscess. Semin Roentgenol 43:168-170, 2008
75. Kagawa R, Okada Y, Shima T, et al: Neuroimaging findings of the development and resolution of solitary brainstem abscess: Characteristics of neuroimagings in the early stage of brainstem abscess and importance of surgical management for brainstem abscess—Case report. Neurol Med Chir (Tokyo) 39:621-624, 1999
76. Hong XY, Chou YC, Lazareff JA: Brain stem candidiasis mimicking cerebellopontine angle tumor. Surg Neurol 70:87-91, 2008
77. Akhaddar A, Mahi M, Harket A, et al: Brainstem tuberculoma in a postpartum patient. J Neuroradiol 34:345-346, 2007
78. Adachi J, Uki J, Kazumoto K, et al: Diagnosis of brainstem abscess in the cerebritis stage by magnetic resonance imaging—Case report. Neurol Med Chir (Tokyo) 35:467-470, 1995
79. Salamon-Murayama N, Russell EJ, Rabin BM: Diagnosis please. Case 17: Hypertrophic olivary degeneration secondary to pontine hemorrhage. Radiology 213:814-817, 1999
80. Guillain G, Mollaret P, de Cas, D: myoclonies synchronies et rythmées vélo-pliaryngo-oculo-diaphragmatiques. Le problème anatomique et physio-pathologique de ce Syndrome. Rev Neurol Paris 2:545-566, 1931
81. Tsui EY, Cheung YK, Mok CK, et al: Hypertrophic olivary degeneration following surgical excision of brainstem cavernous hemangioma: A case report. Clin Imaging 23:215-217, 1999
82. Krings T, Foltys H, Meister IG, et al: Hypertrophic olivary degeneration following pontine haemorrhage: Hypertensive crisis or cavernous haemangioma bleeding? J Neurol Neurosurg Psychiatry 74:797-799, 2003
83. Kitajima M, Korogi Y, Shimomura O, et al: Hypertrophic olivary degeneration: MR imaging and pathologic findings. Radiology 192:539-543, 1994
84. Goyal M, Versnick E, Tuite P, et al: Hypertrophic olivary degeneration: Metaanalysis of the temporal evolution of MR findings. AJNR Am J Neuroradiol 21:1073-1077, 2000
85. Auffray-Calvier E, Desal HA, Naudou-Giron E, et al: Hypertrophic olivary degeneration. MR imaging findings and temporal evolution [in French]. J Neuroradiol 32:67-72, 2005
86. Pearce JM: Palatal myoclonus (syn. Palatal Tremor). Eur Neurol 60: 312-315, 2008
87. Heier LA, Bauer CJ, Schwartz L, et al: Large Virchow–Robin spaces: MR-clinical correlation. AJNR Am J Neuroradiol 10:929-936, 1989
88. Saeki N, Sato M, Kubota M, et al: MR imaging of normal perivascular space expansion at midbrain. AJNR Am J Neuroradiol 26:566-571, 2005
89. Kwee RM, Kwee TC: Virchow-Robin spaces at MR imaging. RadioGraphics 27:1071-1086, 2007
90. Salzman KL, Osborn AG, House P, et al: Giant tumefactive perivascular spaces. AJNR Am J Neuroradiol 26:298-305, 2005